ISSN 1022 - 2502, E-ISSN 2408- 8528
Dhaka Univ. J. Sci. 71(2): 127-133, 2023 (July) DOI: https://doi.org/10.3329/dujs.v71i2.69121

Preparation and Characterization of Carbon Doped ZnO and Its Effectiveness as Photocatalyst under Visible Light

Mahbuba Zaman, Nasrin Akter, Md. Ataur Rahman and Md. Mufazzal Hossain*

Department of Chemistry, Dhaka University, Dhaka-1000, Bangladesh.

(Received : 12 January 2023; Accepted : 20 July 2023)

Abstract

Carbon-doped ZnO (C-ZnO) was prepared and characterized by XRD, SEM, EDX and FT-IR spectroscopy. The substitution of oxygen in the lattice of ZnO by carbon greatly extends its optical sensitivity in the visible light due to the band gap's shrinkage, which promotes the effectiveness of electron-hole separation. SEM images showed that the surface of C-ZnO catalyst is different from that of undoped ZnO. Analysis of the elements present in the sample was done by EDX which affirms that the prepared sample contains Zn, O and C atoms. The existence of ZnO as wurtzite is confirmed by XRD analysis exhibiting little deviation of the peak position due to the presence of carbon in substitutional sites. FT-IR analysis also supports these results. Under visible light irradiation, the prepared C-ZnO shows better photocatalytic efficiency on methylene blue (MB) than un-doped ZnO. The optimum photodegradation efficiency of MB has been observed when 2 percent C-doped ZnO obtained at 300˚C calcination temperature.

Keywords: Dextrose, C-ZnO, MB, photocatalysis, band gap, visible light activity.

I. Introduction

A lot of the textile and leather industries use organic dyes which are the prime polluting sources of water contamination[1]. Water contamination with a variety of organic contaminants is one of the most dangerous challenges facing living beings because these colored organic dyes are mostly carcinogenic and non-biodegradable, creating esthetic pollution, high toxicity, eutrophication, and disturbance to aquatic life cycle[2]. In order to dispel this pollution obstruction in our universe, especially 3rd world countries and developing countries, many researches and laboratory actions have been studied last several decades. Numerous chemical and physical technologies have been proposed for the treatment of wastewater and organic pollutants from the textile industries[3]. When using a physical method, for example, using adsorbent to eliminate organic contaminants along with

dyes, activated carbon is highly helpful[4] but in wide range of application, the reactivation of adsorbent for further usage is not economically fair. Membrane filtration is another method for removing the dyes[5]. However these non-destructive methods result in secondary contamination by shifting the phases of dyes[6]. Furthermore, several non-conventional processes for example ozonation, sodium hypochlorite treatment, electrochemical destruction and radiation processes have some downsides such as ozonation and radiation processes originate hazardous byproducts that may be difficult to expel[7] whereas high chloride level in the water arises from hypochlorite treatment and electrochemical oxidation necessitates a significant supply of power which is costly[8]. Over the last few decades, the most widely used method for oxidizing organic contaminants in domestic and industrial effluent is semiconductor-negotiated photocatalytic oxidation and will be substitutable to traditional processes of environmental cleanup exist because of the capacity to destroy pollutants, wide applicability and environmental friendliness[9]. In the semiconductor-mediated photocatalytic oxidation process, generation of electron-hole pairs occurs when a semiconductor is exposed to photons with energy which is identical to or more than the energy of band gap. These holes and electrons would rejoin or travel to the surface, where they can take part in a number of redox processes, eventually generating reactive species for example $^{\bullet}OH$ radicals, $O_2^{-\bullet}$ and H_2O_2[10] which are powerful oxidizing agents leading to mineralization of organic molecules through non-selective oxidation. The mostly researched and practiced semiconductor is ZnO that has a 3.37 eV band gap energy, a significant binding energy (60 meV) for excitation at ambient temperature, superior electrical as well as optical properties, good environmental stability, strong oxidizing power, nontoxic nature. Moreover, they are relatively cheaper[11]. Due to having all of these properties, ZnO has gained popularity for the use in photodegradation process of various dye pollutants[12]. ZnO, on the other hand, exhibits a significant rate of recombination of photo-generated electron-hole pairs and low optical absorption capacity when exposed to visible light, which limits its application to a great extent. To overcome these drawbacks as well as to develop visible light sensitive ZnO, it must be modified by using several methods such as semiconductor coupling[13], surface organic coating[14], dye sensitization[15], metal or nonmetal doping[16,17] etc. Changes in electrical and optical properties are

*Author for correspondence. e-mail: mufazzal@du.ac.bd

dramatically induced by doping the ZnO lattice with non-metallic elements including carbon, nitrogen, and sulfur resulting in the development of interior energy levels across the band gap, thereby reduces the wide band gap and allowing it to absorb visible light[18]. By doping with carbon, an inherently n-type ZnO is converted into a p-type semiconductor and the prepared material is expected to exhibit enhanced visible light activities[19]. The additional advantage of carbon is that it can channelize the photo-induced electrons to nano-particles of carbon on the catalyst surface that results in the facilitation of the separation of photoelectrons and holes and thereby lessening the recombination rate[20].

Cho et al. [21] claimed that ZnO that had been doped with carbon employing vitamin C as the source of carbon demonstrated an expanded visible light activity. In addition, a number studies shows a better performance for the carbon doped photocatalysts particularly under visible light irradiation.[22-24] In this research, preparation of carbon doped ZnO (C-ZnO) was performed from the cheap and readily available dextrose as a source of C. The characterization and its application as a catalyst for photodegradation of methylene blue (MB) under visible light have been reported. The degradation efficiency of this material is compared with the undoped ZnO.

II. Experimental

Materials

Commercial ZnO was supplied from Sigma-Aldrich, Merck, USA. Merck, Germany provided MB dye and dextrose. The aforementioned compounds were all utilized in analytic grade, requiring no farther treatment. Deionized water was used throughout the whole experiment.

Preparation of C-ZnO

The catalyst, C-ZnO was synthesized[21] with variable carbon doping percentages (1%, 2%, 3% and 4%) in order to make the catalyst of optimum efficiency. The required amount of ZnO, dextrose (as a source of carbon) and deionized water were added while being stirred magnetically. It was constantly swirled and heated at 90˚C using magnetic stirrer in order to minimize the volume of suspension. After that an oven was used to exsiccate the sample at 60˚C. The exsiccated sample was then thrashed, deposited into a porcelain crucible and heated for 4 hours at a specific temperature in a muffle furnace. Calcination temperature was varied between 300˚C to 600˚C.

Photodegradation of MB by C-ZnO

At various experimental conditions, the performances of the prepared catalyst were assessed by measuring the rate of decolorization of MB. In a typical experiment, MB photodegradation was carried out in a 100 mL beaker that served as the reactor. At first, a specific quantity of catalyst and deionized water was taken in this beaker and the suspension was then sonicated for 30 minutes. The addition of higher concentration dye solution to the sonicated suspension was done to achieve a desired concentration. A magnetic stirrer was used to swirl the suspension continuously at dark for 20 min to ensure the adsorption of the dye to reach equilibrium. The suspension was exposed to radiation with constant magnetic stirring. After definite time intervals, the photocatalytic particles were separated from a portion of the irradiated solution by centrifugation, yielding a clear solution for measuring absorbance at the λ_{max} = 664.5 nm of the dye solution. The following equation has been used to compute the percent degradation:

$$\text{Degradation percentage} = \frac{A_o - A}{A_o} \times 100$$

Where, A_o and A are the absorbances of MB solution at time zero and anytime of photodegradation.[25] All of the experiments were carried out under visible light. The visible light source (400-700 nm) composed of five fluorescent lamps which were arranged inside a wooden box. To prevent light absorption, inner surfaces of this box were covered with aluminium foil.

III. Results and Discussion

Characterization by SEM

Scanning electron microscopy (SEM), was used to evaluate the surface pattern of the prepared samples. The shape and size of the particles were observed by employing the images with resolution ×30000. Fig. 1 represents the SEM images of undoped ZnO and C-ZnO that had been

heated at different temperatures between 300˚C and 500˚C. Fig. 1(A) demonstrates that pure ZnO has hexagonal shape with irregularly shaped agglomerated particles. Most of the structure of C-ZnO (calcined at 300°C) is rod-shaped (Fig. 1(B)) whereas SEM images calcined at 400°C reveal a mixture of rod shaped particles and a few number of spherical shaped particles (Fig. 1(C)). However, the images of C-ZnO calcined at 500°C reveals a considerable number of spherical shaped particles together with rod-shaped structure (Fig. 1(D)). Again it is also visually appeared from the images that the particles of C-ZnO are smaller in size than those of undoped ZnO. This means that the doped catalyst has a higher surface area than the un-doped catalyst which is supposed to be more effective in photodegradation process.

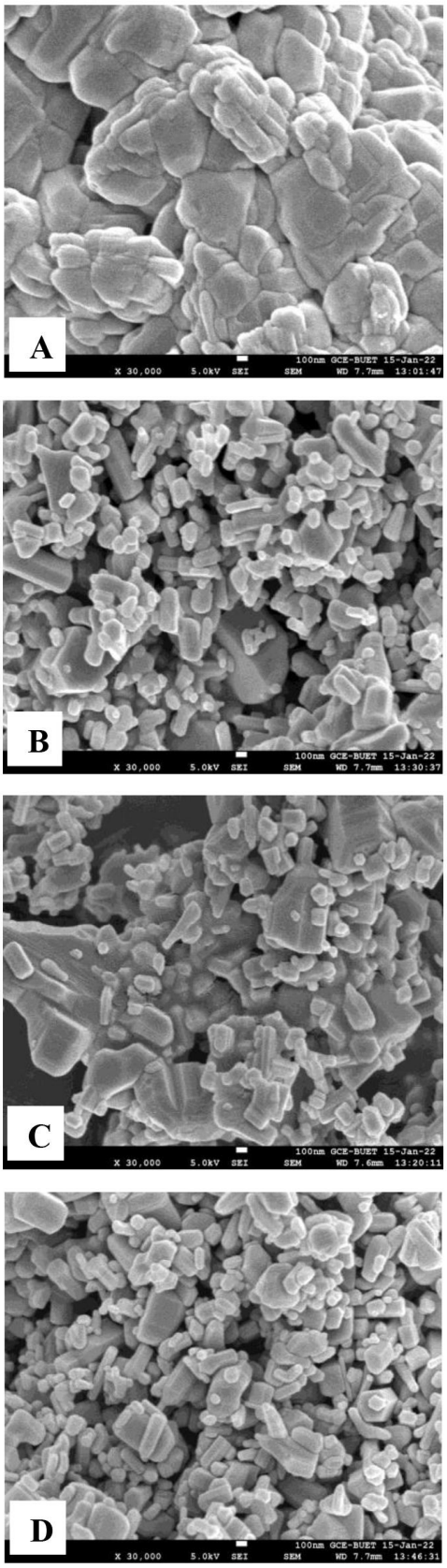

Fig. 1. SEM images of undoped ZnO (A), C-ZnO calcined at 300˚C (B), 400˚C (C) and 500˚C (D).

Characterization by EDX spectroscopy

The conformation of the elements in the experimental samples was accomplished by utilizing energy dispersive X-ray (EDX) spectroscopy and the outcomes are represented in Fig. 2. The existence of carbon, zinc, and oxygen without any other impurities are all corroborated by the EDX spectra of C-ZnO (calcined at different temperatures). However, the exact composition of carbon contained in the matrix of C-ZnO could not be ascertained due to the application a grid coated with carbon in EDX exploration.

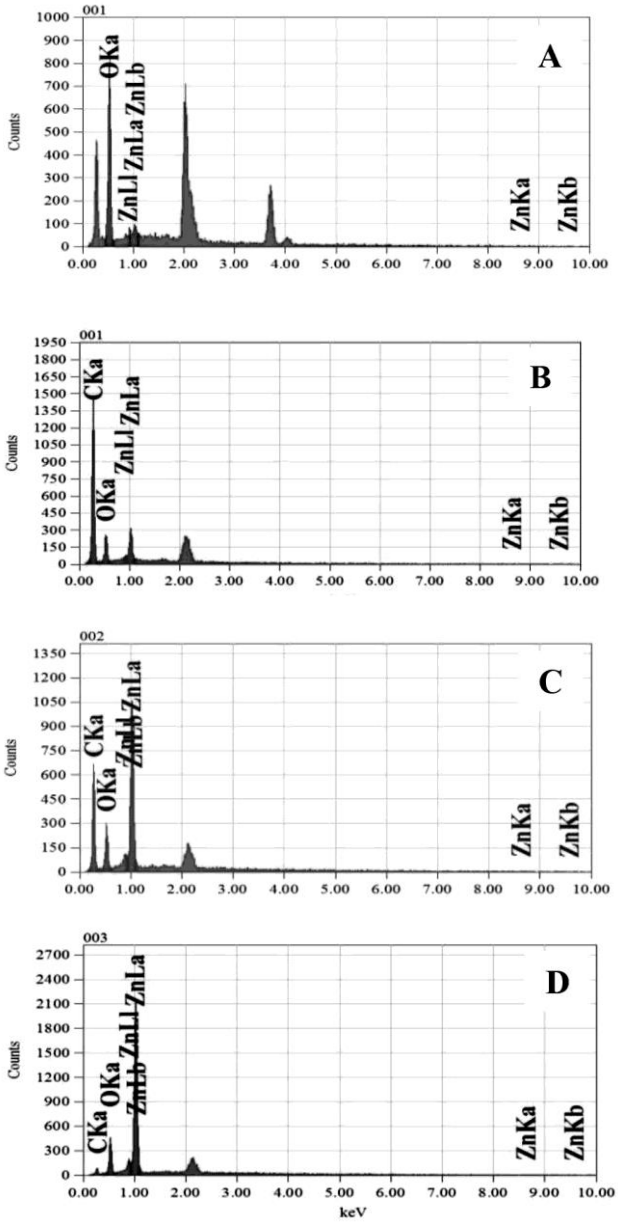

Fig. 2. EDX spectrum of commercial ZnO (A), C- ZnO calcined at different temperatures, 300˚C (B), 400˚C (C) and 500˚C (D).

Characterization by XRD

Fig. 3 displays the X-ray powder diffraction (XRD) patterns of pure commercial ZnO and C-ZnO that has been doped with carbon. The diffraction patterns appear identical to those of ZnO that has hexagonal wurtzite structure (JCPDS 00-005-0664). There was no impurity phases found. It indicates that the perfect wurtzite structure with hexagonal lattice is possessed by C-ZnO. The replacement of O by C would lead to an enlargement of the lattice of C-doped ZnO because carbon has a larger atomic radius (70 pm) than oxygen (60 pm)[26]. The meticulous checking of their XRD patterns supports this aforementioned assumption. Fig. 3 depicts that there is a shift in the diffraction peaks of C-ZnO to a narrower diffraction angle because of lattice enlargement. However, no peak of carbon was observed in the 20-30˚ 2θ range, which could be attributed to a lower carbon contribution.

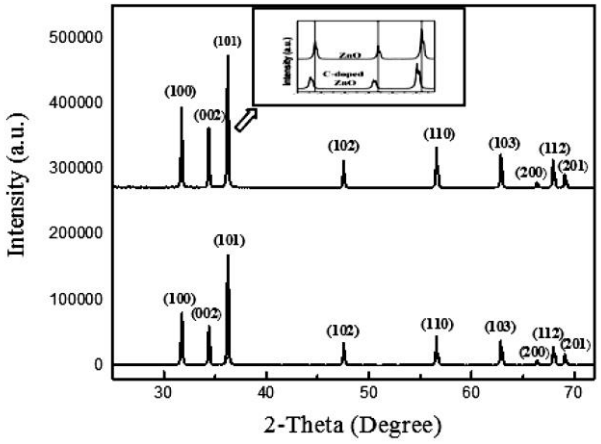

Fig. 3. The XRD patterns of undoped ZnO (above) and C-ZnO (below).

Characterization by FT-IR

Fig. 4 exhibits the Fourier transform infrared spectra (FT-IR) of commercial ZnO together with C-ZnO. A wider band located at 3452.58 cm^{-1} could be assigned to the O-H stretching mode whereas the bending vibrations of O-H bond correspond to the absorption peaks at 1625.99 and 1161.15 cm^{-1}. These peaks guarantee the existence of cramped H_2O on the surface of the catalyst[27,28,29]. The asymmetric and symmetric stretching frequencies of CH_3 are related to the absorption signals at 2924.09 and 2856.58 cm^{-1}. In the zinc oxide lattice, the peak at 426.27 cm^{-1} is due to the stretching vibrational mode of the Zn-O bond[30,31]. Tetrahedral coordination of Zn is responsible for the absorption at 875 cm^{-1}. Possible causes of C-O stretching include absorption peaks at 1384.89 and 1105.21 cm^{-1}.

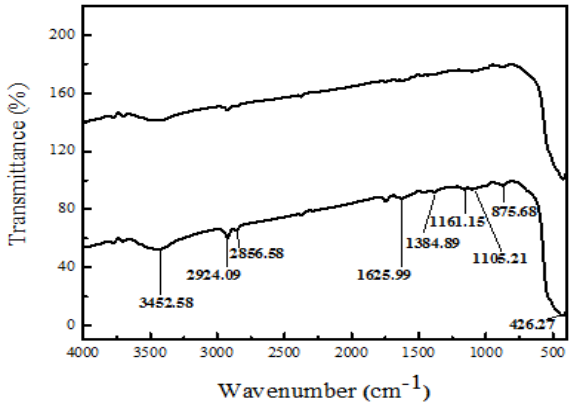

Fig. 4. The FT-IR spectra of undoped ZnO (above) and C-ZnO (below).

Band gap energy determination

Kubelka-Munk theory is used to find out the band gap energy from reflectance measurements.

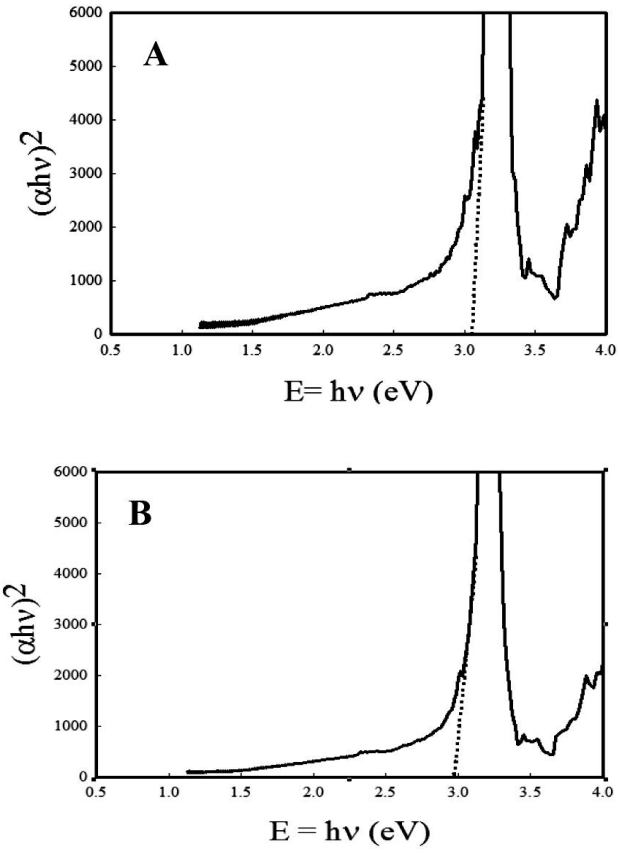

Fig. 5. Plot for the determination of the band gap energies of undoped ZnO (A) and C-ZnO (B).

The energy of band gap is attained by plotting the square product of the absorption coefficient and energy $(\alpha E)^2$ vs energy E, [$(\alpha E)^2$ vs E], where the straight line intersecting

the E axis from the straight segment of the graph represents the band gap energy. By doing this it was found from Fig. 5(A) and 5(B) that undoped ZnO and C-ZnO have band gap energies of 3.10 and 2.96 eV, respectively demonstrating the shrinkage of band gap due to carbon doping. As a result, C-ZnO is expected to have higher photocatalytic performance than undoped ZnO, particularly in the visible region.

Photocatalytic efficiency comparison between undoped ZnO and C-ZnO

In order to compare the photocatalytic activity of prepared material, 1% C-ZnO was used here. For this experiment, the amount of catalyst was 0.20 g/100 mL and the concentration of MB was 3.0×10^{-5} M. Fig. 6 shows that doped ZnO displays higher degradation proficiency compared to un-doped ZnO on exposure to visible light. From band gap energy measurements, it is seen that carbon doping of ZnO causes the band

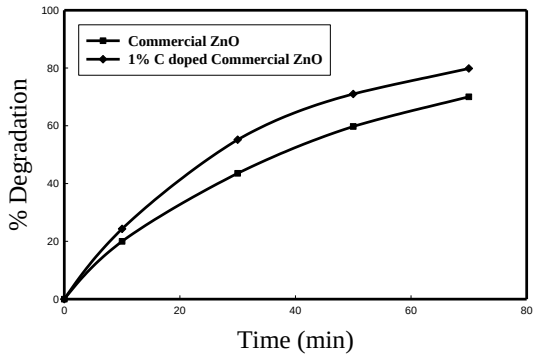

Fig. 6. A plot showing the comparative removal of MB using C-ZnO and un-doped ZnO. Mass of catalyst = 0.20 g, $[MB]_0 = 3.0\times10^{-5}$ M, initial pH =7.30 ± 0.20, light source: visible light.

gap to reduce from 3.10 eV to 2.96 eV. Actually, doping causes the development of energy levels above the valence band, which causes the shrinkage of band gap. As a result, the catalyst's absorption moves towards the visible region from the UV light region. Additionally, carbon reduces the recombination of holes and electrons [32]. Thus under visible light, C-doped ZnO has greater photocatalytic activity than un-doped ZnO.

Effect of different doping percentage of carbon

The effect of various doping percentages in carbon doped ZnO on photodegradation of MB was carried out to determine the optimum doping percentage of carbon that yields the highest degradation efficiency under visible light. In order to accomplish this motive, ZnO doped with 1%, 2%, 3% and 4% carbon were used separately. From Fig. 7, it is seen that the breakdown performance of MB increases from 79.83% to 83.40% with an increase in carbon content from 1% to 2%. Then with a further increase in the doping percentage, the degradation efficiency of MB decreases. It could be attributed to the fact that at first the band gap of ZnO narrows with the increase of carbon content due to incorporation of more intermediate energy levels from carbon and the visible light activity enhances efficiently.

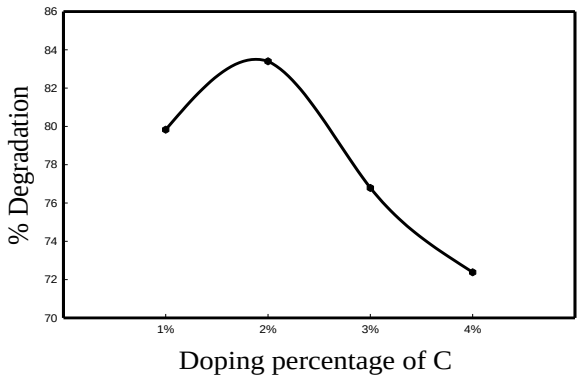

Fig. 7. Effect of doping percentage of C on the percent degradation of MB. Mass of doped catalyst = 0.20 g, $[MB]_0 = 3.0\times10^{-5}$ M, initial pH =7.88 ± 0.03, light source: visible light.

After a certain point, formation of zinc nucleus might occur quickly with carbon and oxygen atoms from the added substrate due to the presence of carbonic species in higher concentrations, resulting in larger particles[33,34]. Thus the surface area decreases and thereby the photocatalytic reaction centers decrease and degradation becomes lower at higher carbon concentration. Another fact is that the higher carbon percentage would operate like a recombination center for the photo-induced electrons and holes and thus there is a reduction in the degradation efficiency.

Effect of various calcination temperature

The temperature was changed between 300°C and 600°C to observe the impact of calcination temperature. It is observed from Fig. 8, that the degradation efficiency diminishes as the calcination temperature increases. It is explicable by the fact that the carbon content in ZnO declines with increasing the calcination temperature. Thereby the band narrowing property also decreases with the increase in calcination temperature and thus gives less degradation efficiency under visible light at higher temperatures.

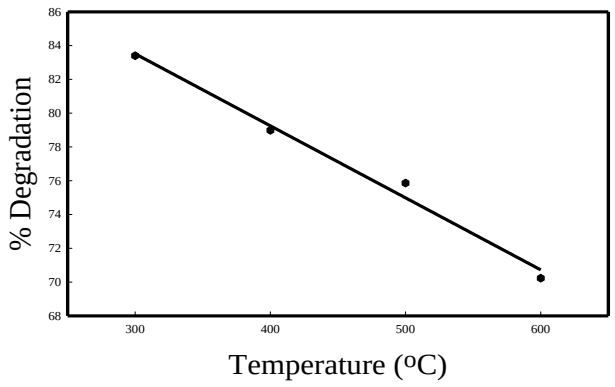

Fig. 8. Impact of calcination temperatures on the photo-degradation of MB. Amount of 2% C-doped ZnO = 0.20 g, $[MB]_0$ =3.0×10^{-5} M, initial pH = 7.28 ± 0.01, light source: visible light.

Photocatalytic mechanism

The catalyst in a photocatalytic reaction absorbs photons with energies higher than or comparable to the energy of band gap which results in the formation of positively charged holes in the valence band as well as negatively charged electrons in the conduction band due to the stimulation of the electrons of the valence band (VB) to the conduction band (CB). These photo-generated holes cause oxidation of H_2O molecules adsorbed on the catalyst surface and create $^{\bullet}OH$ radicals, while electrons reduce dissolved oxygen, resulting in the creation of super oxide anions. These species ($^{\bullet}OH$ and $O_2^{-\bullet}$) can cause MB molecules to undergo photodegradation and produce degraded mineralized products. The mechanism can be represented diagrammatically as follows (Fig. 9):

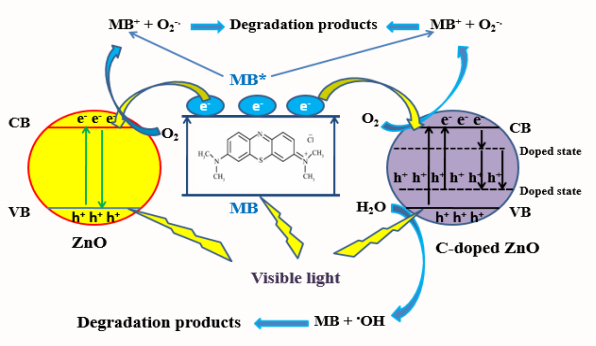

Fig. 9. Mechanism of MB degradation on exposure to visible light.

IV. Conclusion

C-doped ZnO with different percentage of doped C was prepared and characterized using several techniques. The prepared materials have different morphology with smaller particles. The catalytic performance of the prepared materials was tested at different doping percentages of carbon and calcination temperatures by carrying out photodegradation of MB dye under visible light exposure. When exposed to visible light, C-ZnO presented superior and improved photocatalytic activities than un-doped ZnO because of the presence of carbon impurities and defects that cause the band gap to shrink in case of C-doped ZnO. In addition, lower recombination rate of photoelectron-holes pairs by carbon results in improved photocatalytic performance. The most interesting thing of this research is that the developed photocatalyst is more effective in the visible light which should make the degradation procedure cost effective.

References

1. Gao, Q., J. Xu, X. H. Bu, 2019. Recent advances about metal–organic frameworks in the removal of pollutants from wastewater. Coordination Chem. Rev., **378**, 17-31.

2. Li, C., S. Yu, X. Zhang, Y. Wang, C. Liu, G. Chen, H. Dong, 2019. Insight into photocatalytic activity, universality and mechanism of copper/chlorine surface dual-doped graphitic carbon nitride for degrading various organic pollutants in water. J. Colloid and Interface Sci., **538**, 462-473.

3. Ahmed, M. B., A. Kumer, M. Islam, T. S. A. Islam, 2018. The Photochemical Degradation (PCD) of Nitrobenzene (NB) using UV Light and Fenton Reagent Under Various Conditions. J. Turkish Chem. Soc. Sec. A: Chem., **5(2)**, 803-818.

4. Özer, D., G. Dursun, A. Özer, 2007. Methylene blue adsorption from aqueous solution by dehydrated peanut hull. J. Hazardous Mater., **144(1-2)**, 171-179.

5. Liang, C. Z., S. P. Sun, F. Y. Li, Y. K. Ong, T. S. Chung, 2014. Treatment of highly concentrated wastewater containing multiple synthetic dyes by a combined process of coagulation/flocculation and nanofiltration. J. Membrane Sci., **469**, 306-315.

6. Maria, J., 2011. Treatment of textile wastewaters using combinations of biological and physico-chemical methods. Lund University.

7. Ike, I. A., Y. Lee, J. Hur, 2019. Impacts of advanced oxidation processes on disinfection byproducts from dissolved organic matter upon post-chlor (am) ination: A critical review. J. Chem. Eng., **375**, 121929.

8. Lavkulich, L. M., J. H. Wiens, 1970. Comparison of organic matter destruction by hydrogen peroxide and sodium hypochlorite and its effects on selected mineral constituents. Soil Sci. Soc. Am. J., **34(5)**, 755-758.

9. Ma, T. Y., J. L. Cao, G. S. Shao, X. J. Zhang, Z. Y. Yuan, 2009. Hierarchically structured squama-like cerium-doped titania: synthesis, photoactivity, and catalytic CO oxidation. J. Phys. Chem. C., **113(38)**, 16658-16667.

10. Chong, M. N., B. Jing, C. W. K. Chow, C. Saint, 2010. Recent developments in photocatalytic water treatment technology. Water Res., **44(10)**, 2997-3027.

11. Pearton, S. J., D. P. Norton, K. Ip, Y. W. Heo, T. Steiner, 2005. RETRACTED: Recent progress in processing and properties of ZnO. Progress in Mater. Sci., **50(3)**, 293-340.

12. Miah, M. J., M. N. Kayes, M. Obaidullah, M. M. Hossain, 2016. Photodegradation efficiency of prepared and commercial ZnO to remove textile dye from aqueous solution. J. Adv. Chem. Sci., 337-340.

13. Ma, H., J. Han, Y. Fu, Y. Song, C. Yu, X. Dong, 2011. Synthesis of visible light responsive ZnO–ZnS/C photocatalyst by simple carbothermal reduction. Appl. Catal. B: Environ., **102(3-4)**, 417-423.

14. Comparelli, R., E. Fanizza, M. L. Curri, P. D. Cozzoli, G. Mascolo, A. Agostiano, 2005. UV-induced photocatalytic degradation of azo dyes by organic-capped ZnO nanocrystals immobilized onto substrates. Appl. Catal. B: Environ., **60(1-2)**, 1-11.

15. Dong, Z., X. Lai, J. E. Halpert, N. Yang, L. Yi, J. Zhai, D. Wang, Z. Tang, L. Jiang, 2012. Accurate control of multishelled ZnO hollow microspheres for dye-sensitized solar cells with high efficiency. Adv. Mater., **24(8)**, 1046-1049.

16. Anandan, S., M. Miyauchi, 2011. Ce-doped ZnO ($Ce_xZn_{1-x}O$) becomes an efficient visible-light-sensitive photocatalyst by co-catalyst (Cu^{2+}) grafting. Phy. Chem. Chem. Phys., **13(33)**, 14937-14945.

17. Qin, H., W. Li, Y. Xia, T. He, 2011. Photocatalytic activity of heterostructures based on ZnO and N-doped ZnO. ACS Appl. Mater. Interf., **3(8)**, 3152-3156.

18. Liu, S., C. Li, J. Yu, Q. Xiang, 2011. Improved visible-light photocatalytic activity of porous carbon self-doped ZnO nanosheet-assembled flowers. Cryst. Eng. Comm., **13(7)**, 2533-2541.

19. Kochuveedu, S. T., Y. H. Jang, Y. J. Jang, D. H. Kim, 2013. Visible light active photocatalysis on block copolymer induced strings of ZnO nanoparticles doped with carbon. J. Mater. Chem. A., **1(3)**, 898-905.

20. Flores, N. M., U. Pal, R. Galeazzi, A. Sandoval, 2014. Effects of morphology, surface area, and defect content on the photocatalytic dye degradation performance of ZnO nanostructures. RSC Adv., **4(77)**, 41099-41110.

21. Cho, S., J. W. Jang, J. S. Lee, K. H. Lee, 2010. Carbon-doped ZnO nanostructures synthesized using vitamin C for visible light photocatalysis. Cryst. Eng. Comm., **12(11)**, 3929-3935.

22. Srinivasan, N., M. Anbuchezhiyan, S. Harish, S. Ponnusamy, 2019. Hydrothermal synthesis of C doped ZnO nanoparticles coupled with $BiVO_4$ and their photocatalytic performance under the visible light irradiation. Appl. Surf. Sci., **494**, 771-782.

23. Xiao, Y., X. L. Wang, H. Yu, Y. Yang, X. T. Dong, 2021. MOF-5 derived C-doped ZnO decorated with Cu cocatalyst for enhancing visible-light driven photocatalytic hydrogen evolution. J. Phys. Chem. Solids, **149**, 109793.

24. Ansari, S. A., S. G. Ansari, H. Foaud, M. H. Cho, 2017. Facile and sustainable synthesis of carbon-doped ZnO nanostructures towards the superior visible light photocatalytic performance. New J. Chem., **41(17)**, 9314-9320.

25. Yildirim, O. A., H. Arslan, S. Sönmezoğlu, 2016. Facile synthesis of cobalt-doped zinc oxide thin films for highly efficient visible light photocatalysts. Appl. Surf. Sci., **390**, 111-121.

26. Zhou, S., Q. Xu, K. Potzger, G. Talut, R. Grötzschel, J. Fassbender,..., H. Schmidt, 2008. Room temperature ferromagnetism in carbon-implanted ZnO. Appl. Phys. Lett., **93(23)**, 232507.

27. Kumar, S., V. Sharma, K. Bhattacharyya, V. Krishnan, 2016. Synergetic effect of MoS_2–RGO doping to enhance the photocatalytic performance of ZnO nanoparticles. New J. Chem., **40(6)**, 5185-5197.

28. Singh, J., P. Kumar, K. S. Hui, K. N. Hui, K. Ramam, R. S. Tiwari, O. N. Srivastava, 2012. Synthesis, band-gap tuning, structural and optical investigations of Mg doped ZnO nanowires. Cryst. Eng. Comm., **14(18)**, 5898-5904.

29. Gerakines, P. A., W. A. Schutte, J. M. Greenberg, kE. F. van Dishoec, 1994. The infrared band strengths of H_2O, CO and CO_2 in laboratory simulations of astrophysical ice mixtures. arXiv preprint astro-ph/9409076.

30. Samaele, N., P. Amornpitoksuk, S. Suwanboon, 2010. Effect of pH on the morphology and optical properties of modified ZnO particles by SDS via a precipitation method. Powder Technology, **203(2)**, 243-247.

31. Singh, S. C., R. Gopal, 2008. Laser irradiance and wavelength-dependent compositional evolution of inorganic ZnO and ZnOOH/organic SDS nanocomposite material. J. Phys. Chem. C., **112(8)**, 2812-2819.

32. Ashkarran, A. A., 2012. A twice liquid arc discharge approach for synthesis of visible-light-active nanocrystalline Ag: ZnO photocatalyst. Appl. Phys. A., **107(2)**, 401-410.

33. Tan, T. L., C. W. Lai, S. B. Abd Hamid, 2014. Tunable band gap energy of Mn-doped ZnO nanoparticles using the coprecipitation technique. J. Nanomaterials, 2014.

34. Taziwa, R., E. Meyer, D. Katwire, L. Ntozakhe, 2017. Influence of carbon modification on the morphological, structural, and optical properties of zinc oxide nanoparticles synthesized by pneumatic spray pyrolysis technique. J. Nanomaterials, 2017.